**Influence of Shape on the Surface Plasmon Resonance of Tungsten Bronze Nanocrystals**

Tracy M. Mattox[1], Amy Bergerud[1,2], Ankit Agrawal[3], and Delia J. Milliron[1,3]*

[1]The Molecular Foundry, Lawrence Berkeley National Laboratory, Berkeley, CA 94720, [2]Department of Materials Science and Engineering, University of California, Berkeley, CA 94720 and [3]Department of Chemical Engineering, The University of Texas at Austin, Austin, TX 78712.

*milliron@che.utexas.edu

**SUPPORTING INFORMATION**

Crystal structure references are from the Inorganic Crystal Structure Database (ICSD).[1]

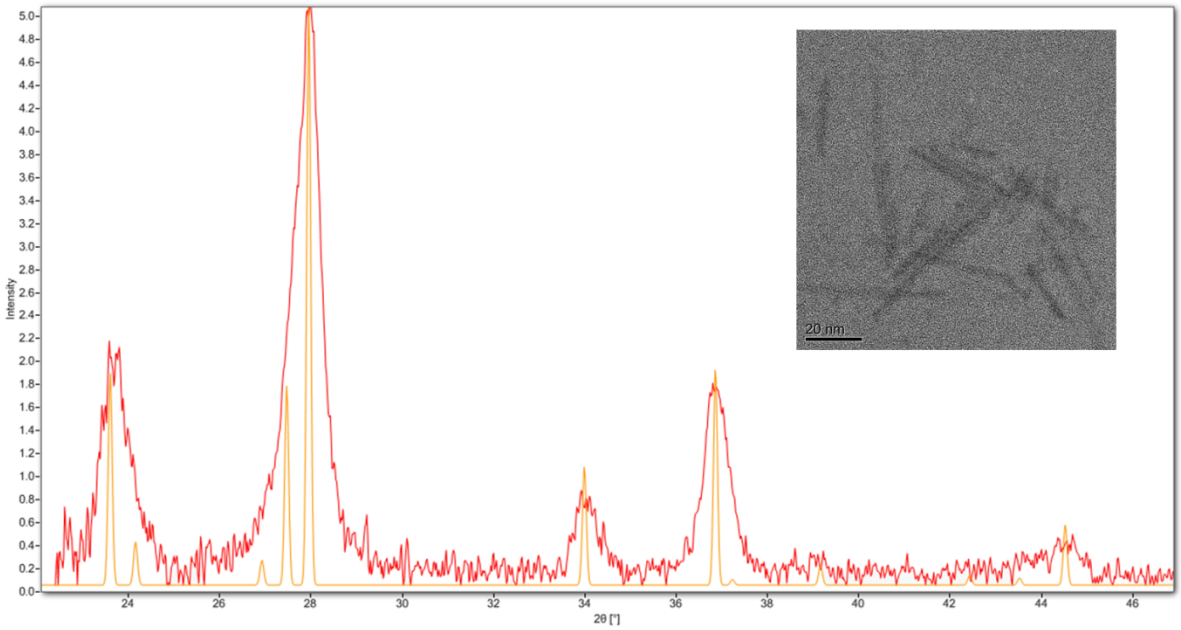


**Figure S1.** XRD of $Rb_{0.29}WO_3$ comparing measured (red) and published data[2] (orange), with inset TEM image of the synthesized nanocrystals**.**

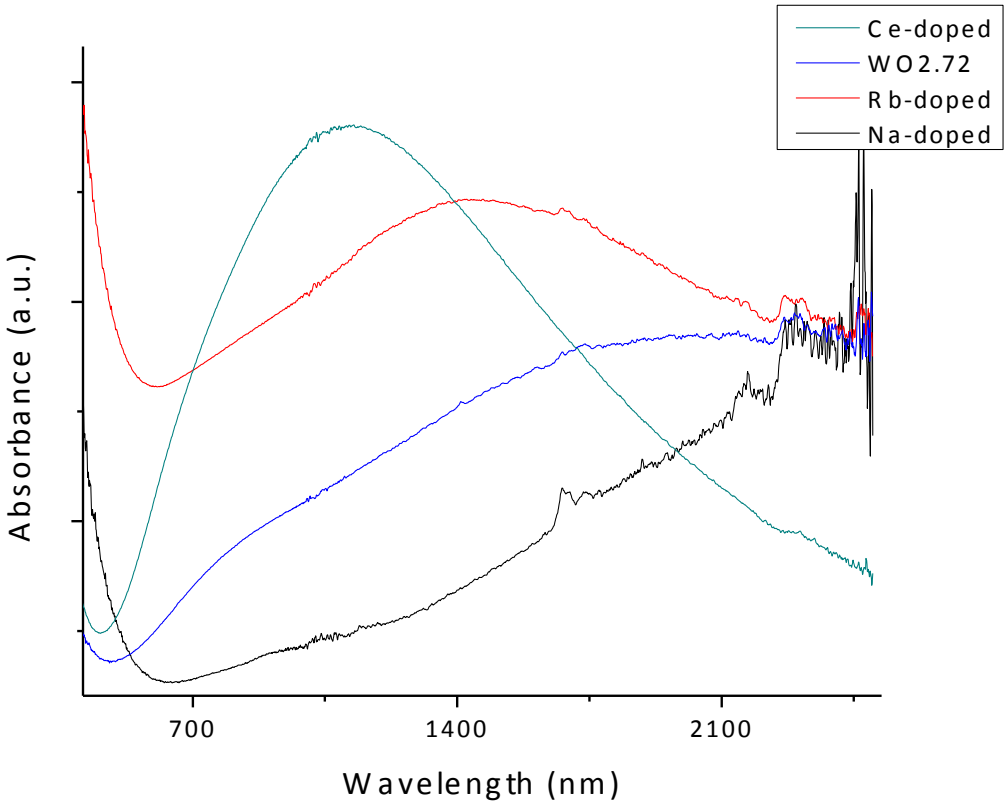


**Figure S2.** Absorbance spectra of $WO_{2.72}$ (structure based on XRD) doped with Rubidium, Sodium, and Cerium.

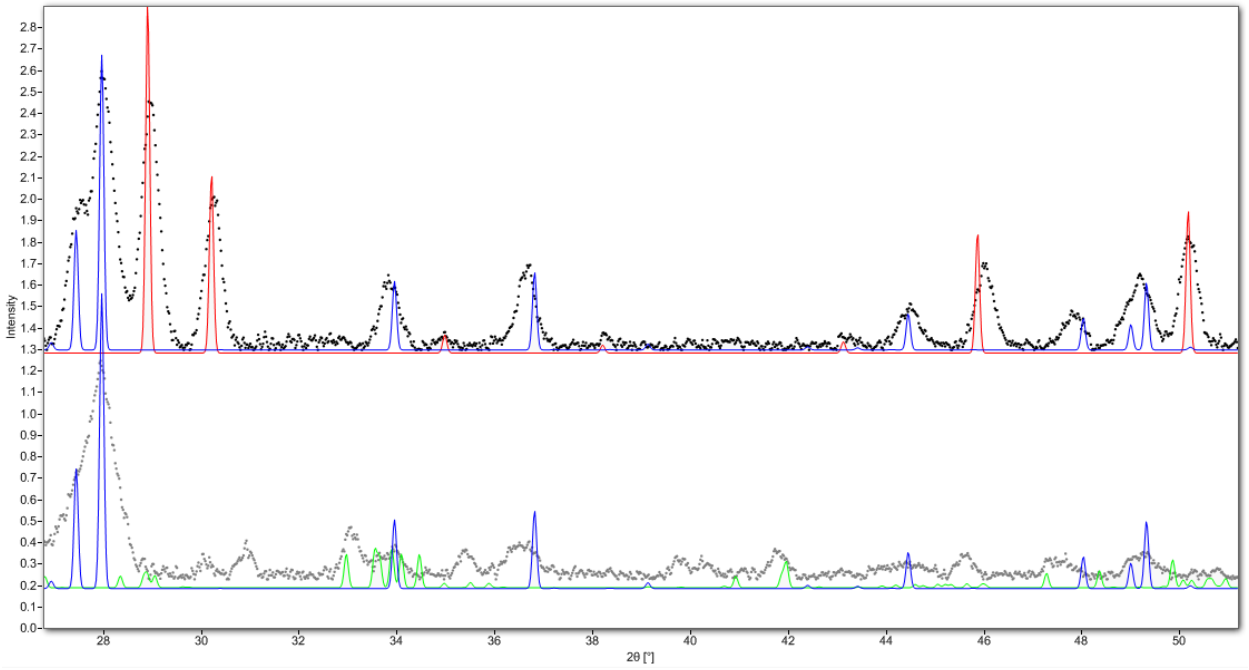


**Figure S3.** XRD of samples synthesized using 0mmol OlAc : 10.6mmol OlAm (top, black dotted line) and 10.6mmol OlAc : 0mmol OlAm (bottom, grey dotted line) with simulated data for $Cs_{0.29}WO_3$ [3] (blue), $CsW_2O_6$ [4] (red), and $WO_3$ [5] (green). The products are not phase pure at these extremes of the surfactant composition.

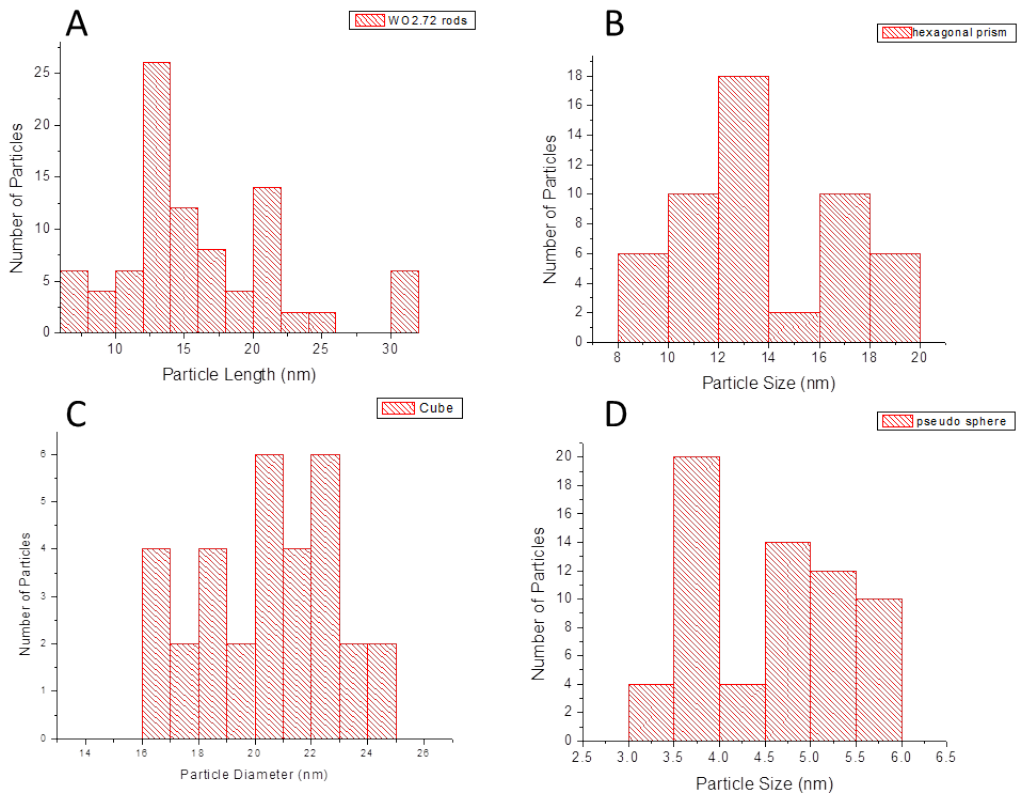


**Figure S4.** Size histograms collected from bright field TEM images including 50-100 particles each of a) $WO_{2.72}$ rods, and $Cs_{0.29}WO_3$ b) hexagonal prisms, c) truncated cubes, and d) pseudo-spheres.

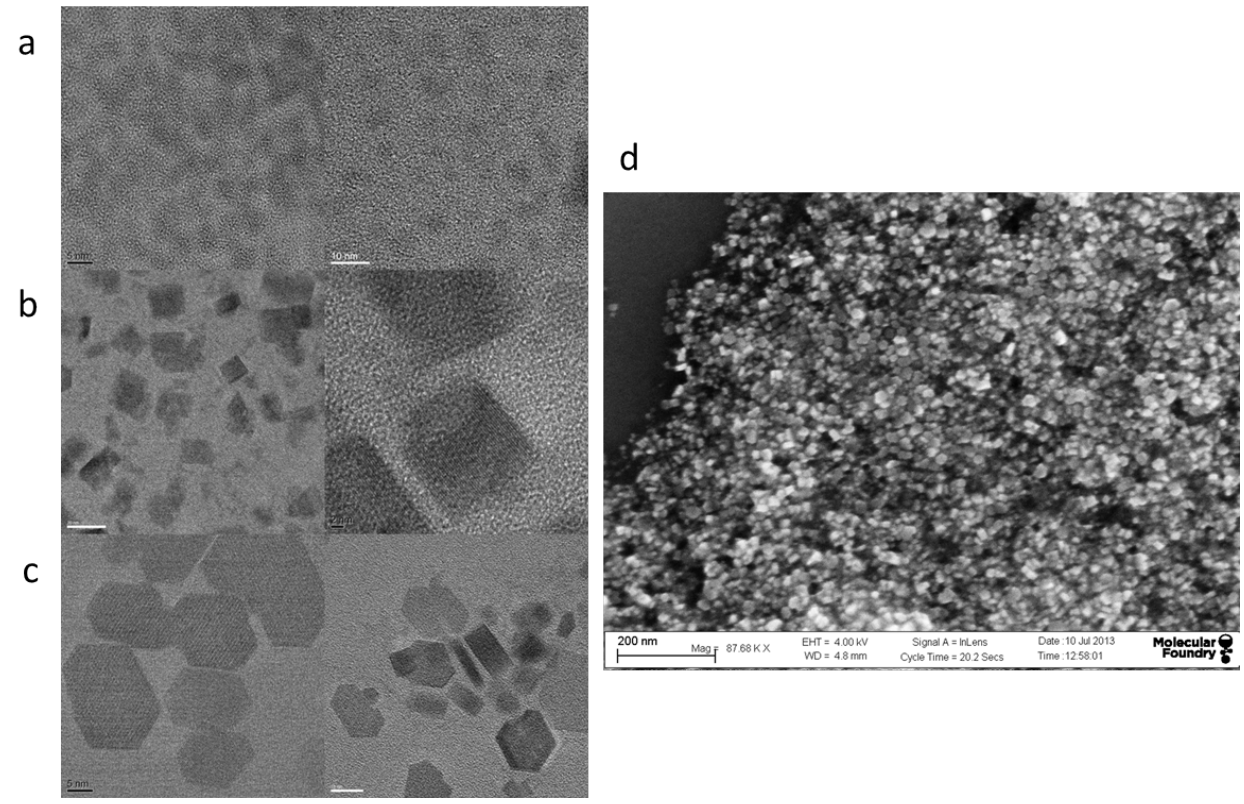


**Figure S5**. Additional TEM images of a) pseudo spheres, b) truncated cubes, c) hexagonal prisms, and d) SEM image of hexagonal prisms.

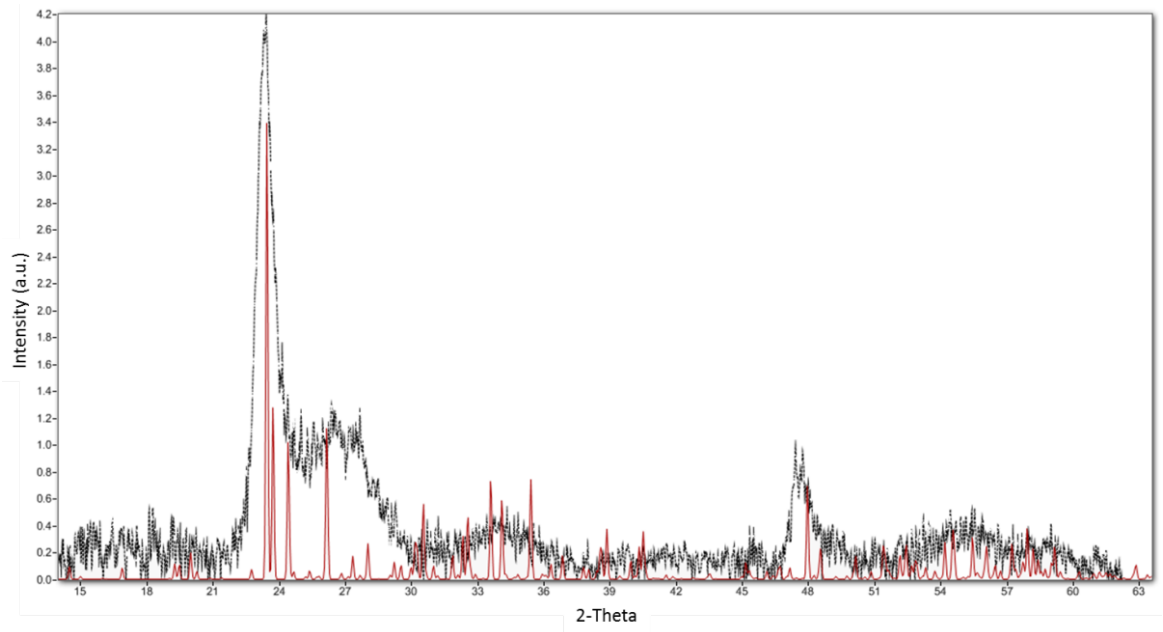


**Figure S6.** XRD of $WO_{2.72}$ (black) and the bulk reference pattern[6] (red).

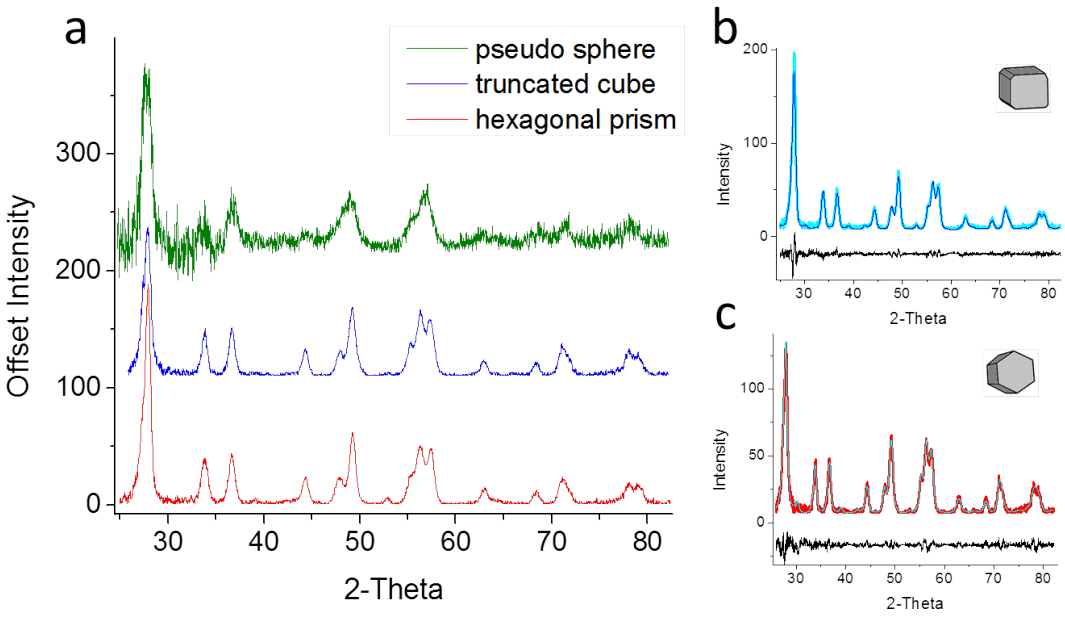


**Figure S7.** Normalized XRD patterns (a) stacked for $Cs_{0.29}WO_3$ spheres, truncated cubes, and hexagonal prisms, and the Le Bail fits with residual plots (black) of a (b) 20.4±2.4nm truncated cubes and (c) 13.2±3.0nm hexagonal prisms. XRD patterns were refined by Le Bail fitting in the GSAS suite for the hexagonal prisms (Rp 0.2091; wRp 0.1101) and truncated cubes (Rp 0.1485; wRp 0.0984). The unit cell increases slightly in size when comparing the truncated cube to the hexagonal prism, with respective increases from 7.395Å to 7.404 Å for a and b and 7.606 Å to 7.615 Å for c.

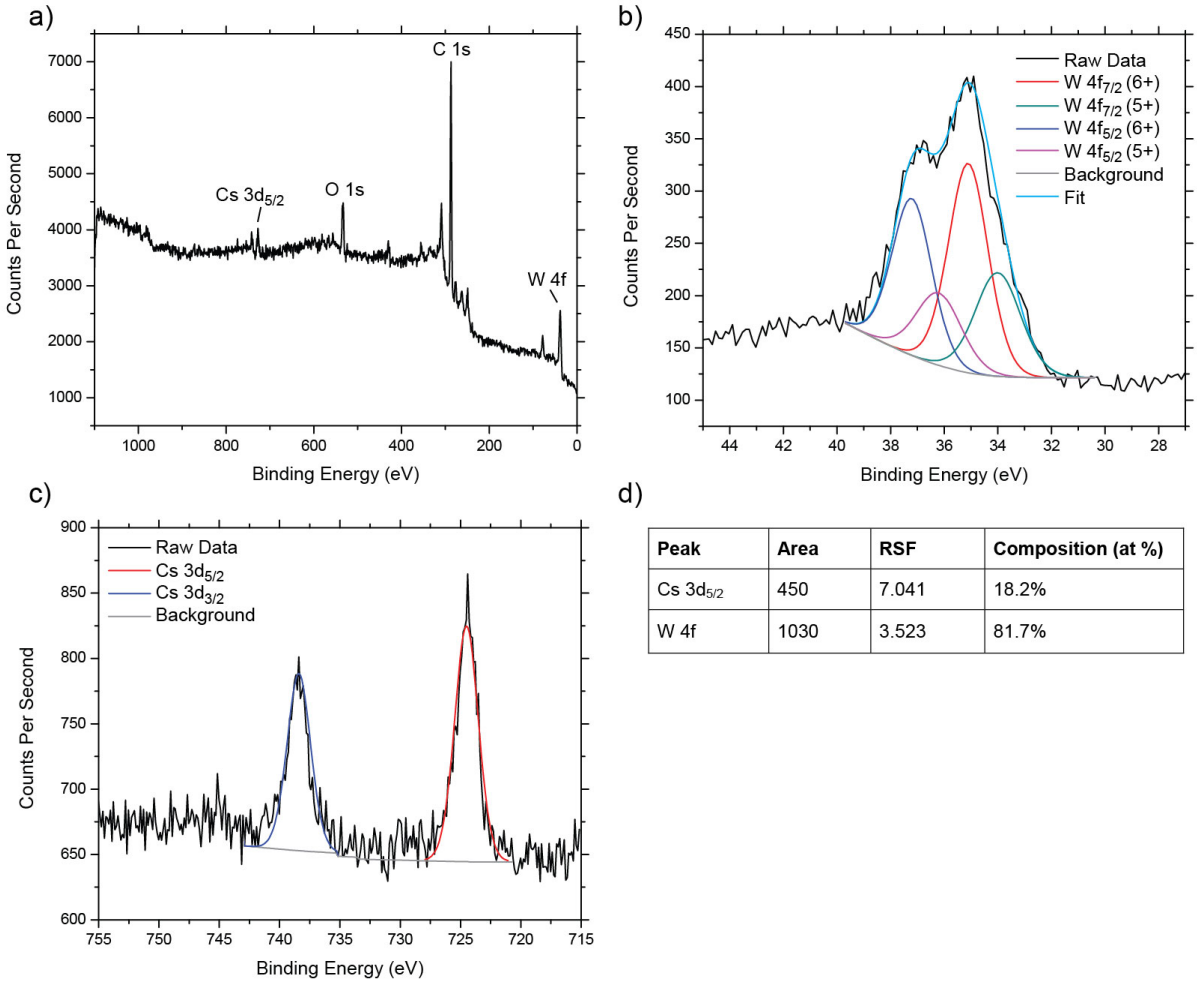


| Peak | Area | RSF | Composition (at %) |
|---|---|---|---|
| Cs $3d_{5/2}$ | 450 | 7.041 | 18.2% |
| W 4f | 1030 | 3.523 | 81.7% |

**Figure S8.** $Cs_xWO_3$ a) XPS survey scan, high resolution scans of b) tungsten $4f_{7/2}$ and $4f_{5/2}$ peaks and c) cesium $3d_{5/2}$ and $3d_{3/2}$ peaks, and d) table detailing peak fit parameters and compositional analysis.

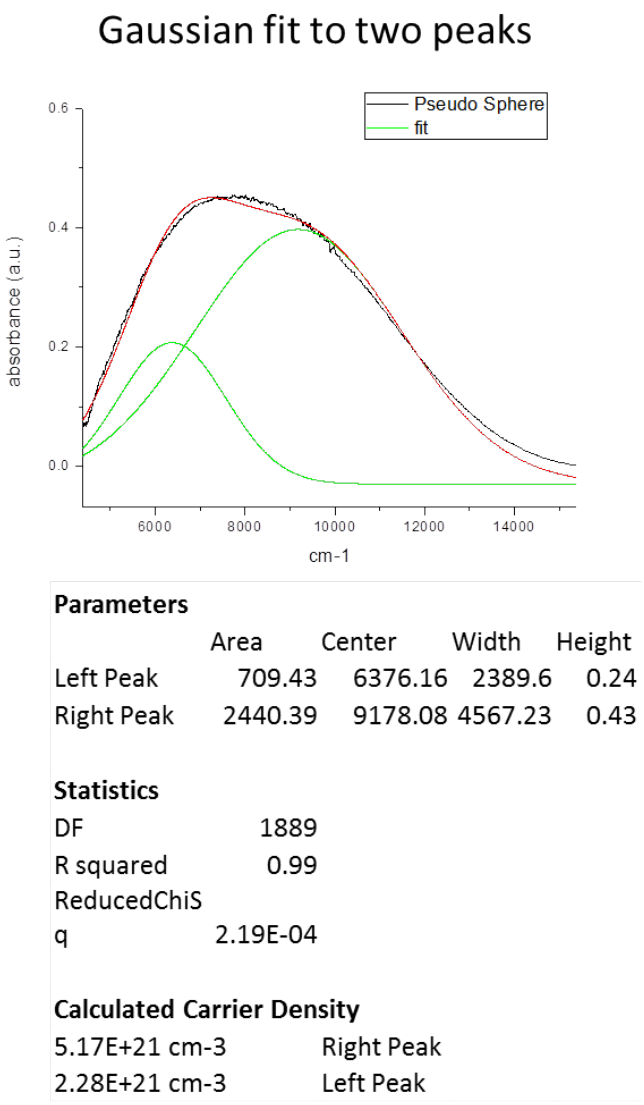


**Parameters**

| | Area | Center | Width | Height |
|---|---|---|---|---|
| Left Peak | 709.43 | 6376.16 | 2389.6 | 0.24 |
| Right Peak | 2440.39 | 9178.08 | 4567.23 | 0.43 |

**Statistics**

| | |
|---|---|
| DF | 1889 |
| R squared | 0.99 |
| ReducedChiSq | 2.19E-04 |

**Calculated Carrier Density**

| | |
|---|---|
| 5.17E+21 cm-3 | Right Peak |
| 2.28E+21 cm-3 | Left Peak |

**Figure S9.** Gaussian peak fit of pseudo sphere absorbance spectra including calculated parameters, statistics, and calculated carrier density.

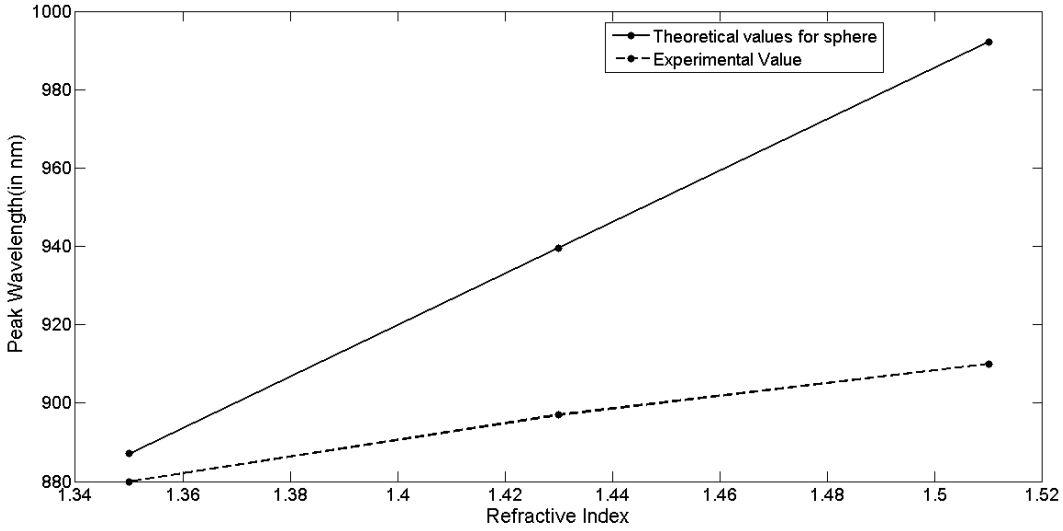


**Figure S10.** SPR peak position of experimental data and the theoretical prediction using Mie's solution to Maxwell's equation plotted against the refractive index of the surround medium (theory) or solvent (experiment).

Analytical expression for the effect of refractive index (RI) of the host medium on SPR peak position[7]:

From the Mie theory, for a nano-sized particle,

$$C_{ext} = \frac{4\pi}{k^2} Re(i(\frac{\varepsilon-\varepsilon_{med}}{\varepsilon+2\varepsilon_{med}})) \quad \text{(eq. 1)}$$

Where $C_{ext}$ is extinction crossection of spherical particle, $k$ is $2\pi n_{med}/\lambda$ where $n_{med}$ is refractive index of medium, $\varepsilon$ is particle dielectric function, $\varepsilon_{med}$ is dielectric function of medium.

From the above expression for resonance,

$$Re(\varepsilon + 2\varepsilon_{med}) \to 0 \quad \text{(eq. 2)}$$

Now since we have spherical particle, from free electron Drude model,

$$Re(\varepsilon) = 1 - \frac{{\omega_p}^2}{\omega^2+\gamma^2} \quad \text{(eq. 3)}$$

Where $\omega_p$ is the plasmon frequency of the bulk metal, $\omega$ is frequency of incident light and $\gamma$ is damping frequency of bulk material.

Since in our case peak frequency lies in the visible range, $\omega \gg \gamma$

$$Re(\varepsilon) = 1 - \frac{{\omega_p}^2}{\omega^2} \quad \text{(eq. 4)}$$

Substituting equation 1 in 4,

$$\omega = \frac{\omega_p}{\sqrt{2\varepsilon_{med}+1}} \quad \text{(eq. 5)}$$

Substituting $\varepsilon_{med} = \eta_{med}^2$, and within a small range of RI, eq. 5 simplifies to

$$\lambda = \sqrt{2}\lambda_p\eta \quad \text{(eq. 6)}$$

Where $\lambda$ is peak wavelength and $\lambda_p$is bulk plasmon wavelength and $\eta$ is refractive index

The above equation shows that for nano-sized spherical particle within a small range of RI, peak wavelength is linearly dependent on RI of the medium.

## REFERENCES


1. Inorganic Crystal Structure Database (ICSD); FIZ Karlsruhe: Germany, 2006.
2. ICSD: 1716.
3. ICSD: 56223.
4. ICSD: 72634.
5. ICSD: 32001.
6. ICSD: 24731.
7. Noguez, C., *J. Phys. Chem C.,* **2007,** *111*, 3806-3819. (b) Noquez, C.; Sanchez-Castillo, A.; Hidalgo, F., *J. Phys. Chem. Lett.*, **2011**, 2, 1038–1044